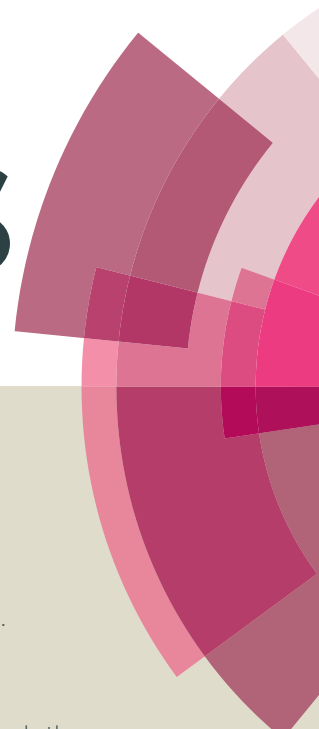


RSC Advances



This article can be cited before page numbers have been issued, to do this please use: M. SELLARO, M. Bellardita, A. BRUNETTI, E. Fontananova, L. Palmisano, E. Drioli and G. Barbieri, *RSC Adv.*, 2016, DOI: 10.1039/C6RA06777H.



This is an *Accepted Manuscript*, which has been through the Royal Society of Chemistry peer review process and has been accepted for publication.

Accepted Manuscripts are published online shortly after acceptance, before technical editing, formatting and proof reading. Using this free service, authors can make their results available to the community, in citable form, before we publish the edited article. This *Accepted Manuscript* will be replaced by the edited, formatted and paginated article as soon as this is available.

You can find more information about *Accepted Manuscripts* in the [Information for Authors](#).

Please note that technical editing may introduce minor changes to the text and/or graphics, which may alter content. The journal's standard [Terms & Conditions](#) and the [Ethical guidelines](#) still apply. In no event shall the Royal Society of Chemistry be held responsible for any errors or omissions in this *Accepted Manuscript* or any consequences arising from the use of any information it contains.



Journal Name

ARTICLE

CO₂ conversion in a photocatalytic continuous membrane reactor

M. Sellaro^a, M. Bellardita^b, A. Brunetti^a, E. Fontananova^a, L. Palmisano^b, E. Drioli^{a,c}, G. Barbieri^{a,*}

Received 00th January 20xx,
Accepted 00th January 20xx

DOI: 10.1039/x0xx00000x

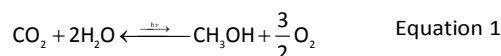
www.rsc.org/

The reduction of CO₂ with water by using photocatalysts is one of the most promising new methods for advancing in CO₂ conversion to valuable hydrocarbons, as methanol. In this work, prepared TiO₂-Nafion-based membranes were used in a photocatalytic membrane reactor, operated in continuous, for converting CO₂ in methanol. By using the membrane with the best TiO₂ distribution, a MeOH flow rate/TiO₂ weight of 45 μmol (g_{catalyst} h)⁻¹ was measured operating at 2 bar of feed pressure. So far, this value results to be higher than the most of the literature data reported up to date. Moreover, MeOH production is considered as a relevant advance over the existing literature results mostly proposing CH₄ as reaction products.

Introduction

One of the main responsible of global climate change is greenhouse gases emission with ca. 36 Gton of CO₂ emitted per year by both natural sources, including decomposition and human sources such as burning of fossil fuels like coal, oil and natural gas, cement production, deforestation, etc.¹ Today, many efforts and, in some cases, with a good level of success, have led to the concretization of capture processes able to separate CO₂ from the rest of the emitted gaseous streams with a targeted level of purity, together with a minimal energy penalty.² However, the main hurdle remains the final destination of these huge CO₂ streams. If, from one hand, storage results as the most likely option, on the other hand the identification of new environmentally improved routes and methods enabling to reduce the emissions of such a compound and to obtain new sustainable energy sources is a key challenge, which would have a significant environmental impact. To this purpose, new greener technologies were studied and developed, especially to convert CO₂ into useful chemical species and fuels.^{3,4} Actually, converting CO₂ to valuable hydrocarbons seems to be one of the most recent advances in CCU (Carbon Capture and Utilization), being one of the best solutions to both global warming and energy lack problems. The reduction of CO₂ with water to fuels by using photocatalysts is one of the most promising methods to be investigated, as it represents a greener process and an attractive route from an economic and environmental point of view. CO₂ can be converted by irradiating it with UV light at room temperature and ambient pressure and thus solar energy could be directly transformed and stored as chemical energy.^{5,6}

Therefore, the photoreduction of CO₂ to chemicals, such as methane and methanol, results to be very interesting. In particular, the main interest is addressed to the production of methanol, as it can be easily transported, stored and used as gasoline-additives, as well as transformed to other useful chemicals by means of classic technologies.⁵ Inoue et al.⁷ firstly reported about the production of HCOOH, HCHO and trace amounts of CH₃OH from the reduction of CO₂ with H₂O under irradiation of aqueous suspensions of semiconductor powders such as TiO₂, whereas the photocatalytic production of CH₄ from CO₂ was firstly reported by Hemminger et al.⁸ Nevertheless, this technology presents some difficulties related to non-effective catalysts, low yield and selectivity. From a thermodynamic perspective, CO₂ conversion with water into methanol and oxygen (Eq. 1) is endoergonic, the Gibbs molar free energy being 698.7 kJ mol⁻¹ at 298 K.



In order to improve the efficiency of the reaction, many research efforts were directed to the development of several new types of photocatalysts.⁹ However, among all the applied photocatalysts, TiO₂ results one of the most used materials for the photocatalytic conversion of CO₂ into fuels, owing to its chemical inertness, no-photocorrosion, stability against photoirradiation, suitable optical and electronic qualities, low cost and commercial availability, as well as no-toxicity.¹⁰ TiO₂ anatase and rutile band gaps are located at about 3.2 eV and 3.0 eV, respectively and the best photocatalytic efficiency can be obtained using anatase with a small admixture of rutile (approximately 75% anatase and 25% rutile).^{10,11} However, in addition to the nature of the photocatalyst to be used, one should consider also that the photocatalytic conversion of CO₂ is a surface reaction involving two important stages: (1) CO₂ adsorption to the catalyst surface and (2) CO₂ decomposition under UV irradiation in the presence of

^aInstitute on Membrane Technology (ITM-CNR), National Research Council, c/o the University of Calabria, Cubo 17C, Via Pietro Bucci, 87036 Rende CS, Italy

^bDepartment of Energy, Information Engineering and Mathematical Models (DEIM), University of Palermo, Viale delle Scienze, 90128 Palermo PA, Italy

^cDepartment of Environmental and Chemical Engineering, University of Calabria, Cubo 44A, Via Pietro Bucci, 87036 Rende CS, Italy

reductants. Therefore, the mass transfer rate of CO₂ and the catalyst surface area are other two important parameters to be controlled to improve the photocatalytic efficiency. As a consequence, catalyst configuration during the photochemical reaction is of high concern to increase the products yield.

The immobilization of the catalyst into polymeric membranes as supports and, thus the use of a membrane reactor for this type of reaction, can be an interesting and valid solution to be adopted. Membrane reactor use takes several advantages such as a better exposition of catalyst to UV light to carry out the reaction, the tailoring of reactants and catalyst contact, the reduction of catalyst aggregates formation, an easier recovery of the catalyst which can be so simply reused, a better control of fluid-dynamics. Moreover, polymeric membranes are easily handled and imply lower costs with respect to other inorganic supports.

Up to now, many works developed photocatalytic membranes with TiO₂ deposited on or entrapped in membranes,¹²⁻¹⁷ especially for water purification or wastewater treatment in advanced oxidation processes, for reduction reactions,¹⁸⁻¹⁹ and also some pilot-plant experiments were carried out as in the case of the PHOTOPERM[®] process for phenol and other organics degradation.²⁰⁻²² Leong et al.²³ have recently proposed a review about the types of membrane as supports and related photocatalytic membrane preparation and characterization, focusing on the application of TiO₂ photocatalytic membranes for removal of pollutants contained water.

TiO₂ can be successfully supported on perfluorinated ionomer membranes, taking advantage of the superior chemical stability and the optical quality of the membrane itself. In many cases, Nafion is the most studied perfluorinated material and several studies were performed on the use of Nafion thin films or membranes as a support for metal or semiconductor particles.^{24,25} It was demonstrated that Nafion can be useful not only as a support to fix semiconductor particles but also as a stabilizing agent for semiconductor microcrystalline colloids.²⁶ Nafion is constituted by an extremely hydrophobic perfluorinated hydrocarbon backbone and several side-chains with fixed sulfonic end groups able to interact with charged/polar species by electrostatic interactions and hydrogen bonds.²⁷ In this way the polymer conjugates a high stability under quite harsh conditions, including UV irradiation, with a high affinity for charged/polar catalyst, as well as it offers a functional microstructured environment that can have a positive influence on the transition states and reaction kinetics for the formation of polar products.²⁸ Moreover, as it is also reported in literature, no change of the band gap are expected when TiO₂ is incorporated in the Nafion.¹⁹ Miyoshi et al.²⁶ prepared TiO₂ microcrystallites in Nafion, adding an alcoholic Nafion solution to TiO₂ colloids. The obtained TiO₂/Nafion in wet form was then used for photodecomposition of acetic acid into CH₄ and CO₂. In many cases, TiO₂ is incorporated in Nafion commercial membranes by soaking them in a solution of Ti-precursor and then treating the Ti-loaded films for obtaining the formation of TiO₂ particles.^{24, 29, 30} As regards CO₂ conversion, in 1997,

Premkumar and Ramaraj³¹ prepared metal porphyrin and phthalocyanine adsorbed Nafion membranes to be used for the photocatalytic reduction of CO₂ to formic acid. More recently, Pathak et al.³² immobilized TiO₂ nanoparticles in porous cavities of commercial Nafion membranes, soaking them in an isopropanol solution of Ti(OC₃H₇)₄ and then immersing the obtained films in boiling water to form TiO₂ nanoparticles by hydrolysis. They found out that the homogeneous dispersion of the photocatalyst in Nafion thin films allowed the photoreduction of CO₂ under optically homogeneous reaction conditions, with consequent improved conversion. In a typical experiment, they filled an optical cell, containing the photocatalytic film, with supercritical CO₂ to a final pressure of 138 bar (2000 psi). After irradiation through a water filter for 5 h, the production of formic acid, together with methanol and acetic acid was observed. Subsequently, Pathak et al.³³ performed other catalytic tests using TiO₂-loaded Nafion membranes coated with silver metal via photolysis and in which the major reaction product was methanol.

In this work, photocatalytic Nafion membranes were prepared by immobilizing bare TiO₂, previously synthesized from TiCl₄ as precursor, into the polymeric matrix. Both the catalyst powder and then the photocatalytic membranes obtained were characterized by means of different techniques. Finally, the membranes were tested in order to verify their catalytic efficiency for CO₂ photoreduction with water for obtaining methanol, under UV-Vis irradiation in a continuous reactor. At the best of our knowledge, this work is the first example of photocatalytic reactor operated in continuous for CO₂ photoreduction using dense mixed matrix TiO₂-based Nafion membranes.

Experimental

Catalyst preparation

TiO₂ sample was prepared by using titanium(IV) chloride (TiCl₄, Fluka 98%) as the starting material. TiCl₄ was added under stirring at room temperature to distilled water in the molar ratio Ti/H₂O 1:60 and a good dispersion was obtained. After ca. 12 h of stirring it turned in a clear solution that was boiled for 2 h under agitation. This treatment produced a milky white TiO₂ dispersion that was dried under vacuum at 323 K.

Catalyst characterization

XRD pattern of the powder was recorded at room temperature by an Itai Structures APD 2000 powder diffractometer using the CuK- α radiation and 2 θ scan rate of 2°/min. The crystallite sizes was evaluated by means of the Scherrer equation: $\Phi = K\lambda/(\beta \cos \theta)$, where Φ is the crystallite size, λ is the wavelength of the X-ray radiation (0.154 nm), K is usually taken as 0.89, β is the peak width at half maximum height after subtraction of the equipment broadening and $\theta=12.65^\circ$ for TiO₂ anatase and $\theta=13.70^\circ$ for TiO₂ rutile. The phase content (%) was calculated using the formula:

$$W_R = A_R / (K_A A_A + A_R)$$

Table 1. Membrane preparation conditions

Membrane	1	2	3	4
Solvent in solution, wt%	97.80		97.72	97.83
Polymer in solution, wt%	2.173		2.172	2.174
Catalyst in solution, wt%	0.027		0.109	0
Solvent	MeOH:H ₂ O (50:50 wt%)	EtOH:H ₂ O (50:50 wt%)	EtOH:H ₂ O (50:50 wt%)	MeOH:H ₂ O (50:50 wt%)
Catalyst in membrane, wt%	1.2	1.2	5	0

Where W_R indicates the content of Rutile, A_A and A_R the integrated intensities of Anatase (101) and Rutile (110) peaks, respectively, and K_A is a coefficient equal to 0.884^{34} .

The specific surface area of the sample was calculated in a Flow Sorb 2300 apparatus (Micromeritics) by using the single-point BET method. The sample was degassed for 0.5 h at 250 °C prior to the measurement. SEM observations were obtained using a Philips XL30 ESEM microscope, operating at 25 kV on specimens upon which a thin layer of gold was evaporated.

UV-Vis spectra of the photocatalyst were obtained by diffuse reflectance spectroscopy (DRS) using a Shimadzu UV-2401 PC instrument. BaSO₄ was used as a reference sample and the spectra were recorded in the range 200-800 nm. Band gap value was determined by plotting the modified Kubelka-Munk function, $[F(R'_{\infty})/hv]^{1/2}$, versus the energy of the exciting light.

Membranes preparation

Nafion™ (Fig. 1) 5 wt% solution was purchased by Quintech e.K. – Brennstoffzellen Technologie (Germany). Methanol and ethanol were purchased from VWR Prolabo Chemicals (USA). Distilled water was used as a co-solvent for the membranes preparation. The flat sheet Nafion membranes were prepared by using the casting and solvent evaporation technique. Two types of membrane were prepared: a bare Nafion membrane (0 wt% of catalyst) and photocatalytic Nafion membranes, containing the TiO₂ catalyst. In the general procedure adopted, as a first step, the polymer contained in the commercial 5 wt% solution was recovered by solvent evaporation at 80°C under magnetic stirring. Then the polymeric solution for the membranes preparation was obtained by adding to the recovered polymer the solvent mixture (MeOH:H₂O or EtOH:H₂O, 50:50 wt%, Table 1) under magnetic stirring and at room temperature.

For the photocatalytic membranes preparation (Membrane 1, 2 and 3), after a complete polymer dissolution, the catalyst was added to the obtained solution and the resulting dispersion was left under stirring for 1 hour more. Then it was sonicated for 30 minutes more in order to favour the homogenization.

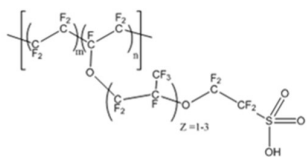


Fig. 1. Nafion molecular structure

The catalyst and polymer dispersion obtained was then casted in the Petri dish and the solvent evaporation was carried out in the climatic chamber. In the case of blank Membrane 4, the same procedure was followed but without catalyst dispersion. For membrane 1 and 4 the temperature of the climatic chamber was 60±4; for Membrane 2 and 3 was 68±4. For all the membranes samples prepared the relative humidity of the climatic chamber was fixed at 12±5% and the solution volume cast in the Petri dish was selected in order to have an initial liquid layer thickness of 5 mm.

The membrane surface exposed to air during evaporation step was indicated as UP; whereas the surface in contact with the Petri dish was indicated as DOWN. After solvent evaporation, both the two types of membranes (photocatalytic and blank) underwent heat treatment at 120°C for residual solvent removal. Then the flat sheet membranes obtained were detached from the Petri dish with a little water quantity and then dried at room temperature. The mean membrane thickness was of 75±5 micrometers.

Membranes characterization

The obtained membranes were characterized by different techniques. The cross-section and surface morphology was observed by scanning electron microscopy (SEM) using a FEI Quanta 200 Philips SEM instrument. Cross-sections were prepared by fracturing the membrane in liquid nitrogen. The samples were “metallized” with graphite. The distribution of heavy elements into the catalytic membranes was observed by using the imaging of a back-scattered electron (BSE) in addition to the secondary electron (SE) detectors.

A Perkin Elmer Spectrum One was utilized for FT-IR spectroscopy analyses in attenuated total reflectance (ATR) of both UP and DOWN membrane surfaces. The diffuse reflectance UV-Vis spectra were recorded with a Perkin Elmer LAMBDA 650 spectrophotometer operating with a 60 mm Integrating Sphere in a wave length range between 250 and 800 nm. The correspondent reflectance spectra were processed and reported as absorbance spectra in Kubelka-Munk units.

Photocatalytic reaction measurements

The photocatalytic membranes were utilized in CO₂ photoreduction with H₂O as the reducing agent.

A medium-high mercury vapour lamp with emittance from 360 nm (UVA) to 600 nm, (Zs lamp by Helios Italquarz, Milan) was used for irradiating the membranes. The runs were carried out by placing the membranes into a flat sheet membrane module equipped with a quartz window, allowing the UV radiation to

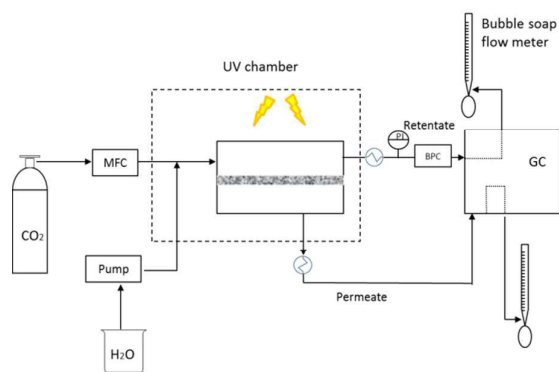


Fig. 2. Scheme of the experimental apparatus

get to the catalytic membrane surface (active membrane area 19.2 cm²).

The membrane module was placed in an UV exposition chamber where a stream of CO₂ was continuously fed by means of a mass flow controller. A water stream was also fed by means of an HPLC pump. The H₂O:CO₂ feed molar ratio was 5:1. The trans-membrane pressure difference was regulated by a back pressure controller and set at 2 bar. Fig. 2 shows the scheme of the experimental apparatus. The membrane reactor consists mainly of three parts: the feed/retentate chamber, the permeate volume and the catalyst loaded membrane. The two reactor chambers can be considered as lumped parameters systems since no concentration gradient of any chemical species is expected owing to also the low conversion of this specific reaction. Inside the membrane, species concentration gradients along the membrane thickness, even though very small, are expected owing to permeation and reaction.

The reaction performance was evaluated through MeOH yield and flow rate/TiO₂ weight calculated accordingly to Eq. 2 and 3, respectively.

$$\text{MeOH yield} = \frac{\text{MeOH}_{\text{out}} \text{ flow rate}}{\text{CO}_2 \text{ feed flow rate}}, \frac{\text{mol min}^{-1}}{\text{mol min}^{-1}} \quad \text{Equation 2}$$

$$\text{MeOH production rate} = \frac{\text{MeOH}_{\text{tot}} \text{ flow rate}}{\text{Catalyst mass}}, \frac{\text{mol min}^{-1}}{\text{g}} \quad \text{Equation 3}$$

Before the photocatalytic experiments with CO₂ as substrate, all of the membranes were subjected to “blank reaction” measurements. In this case, together with H₂O, an argon stream was fed into the reaction module instead of CO₂, in continuous for 8-12 h in the same operating conditions chosen for the catalytic experiments including UV-Vis irradiation (Table 2). The aim of this procedure was to clean the membrane from residuals of solvent and other low molecular weight organics eventually present in the polymer solution that could be released during the reaction test contaminating the reaction mixture.

Table 2. Operating conditions for reaction measurements

CO ₂ (or Ar) flow rate, mL(STP) min ⁻¹	20
H ₂ O _{liquid} , mL min ⁻¹	0.079
H ₂ O : CO ₂ (or Ar) molar ratio	5:1
Feed Pressure – Permeate Pressure, bar	2
Temperature, °C	45±5

Both the retentate and permeate streams outgoing the reactor were condensed by means of an ice bath (0°C). Then the incondensable species in both cases were sent to bubble soap flow meters, in order to evaluate the correspondent flow rate. Moreover, the composition of these streams was measured by an Agilent Technologies 7890A gas chromatograph with TCD (HP-PLOT and Molsieve columns). The condensate components of the retentate and permeate were also periodically sampled and analysed by means of an Agilent Technologies 6890N gas chromatograph with FID (HP-5 column).

Ionic species were determined by ionic chromatography using a Dionex DX 120 instrument equipped with an Ion-Pac AS14 4mm column (250 mm long, Dionex). The eluent was an aqueous solution of NaHCO₃ (8 mM) and Na₂CO₃ (1 mM). Each membrane was characterized for 15 hours, allowing, anyway, to get the desired information. No catalytic and blank measures were carried out during the night and, thus, for longer times. In the case of blank reaction measurements, the liquid samples withdrawn were subjected to TOC (total organic carbon) measurements, by means of a TOC-VCSN Shimadzu analyser, to evaluate the possible presence of organic contaminants in polymer solution, residual solvent or Nafion fractions at low molecular weight. TOC was measured only during blank (no-reaction; Ar+H₂O as feed) tests confirming the stability under irradiation of Nafion membranes since its values decreased with the time.

If not otherwise specified, the membrane was placed into the module exposing toward the quartz window (i.e. the retentate side) its UP surface. In the first case, the membrane was placed into the module exposing to the retentate side its UP surface; in the second one the DOWN (or “Petri side”) surface, richer in catalyst, was exposed. Membrane 2 and 3 were tested just exposing their UP surfaces to reactants and UV light.

Results and discussion

Photocatalyst characterization

The diffraction pattern of TiO₂ sample (Fig. 3a) identifies a mixture of the anatase and rutile polymorphs with a slight degree of crystallinity owed to the low synthesis temperature. Fig. 4 shows the diffuse reflectance spectra of the prepared sample: the strong absorption in the range 300–380 nm corresponds to the charge transfer process from O 2p to Ti 3d. TiO₂ is an indirect semiconductor so that its band gap energy can be determined from the tangent lines to the plots of the modified Kubelka-Munk function, $[F(R'_{\infty})/hv]^{1/2}$, versus the energy of the exciting light, as shown in the inset of the Fig.. Some features of the TiO₂ sample are listed in Table 3.

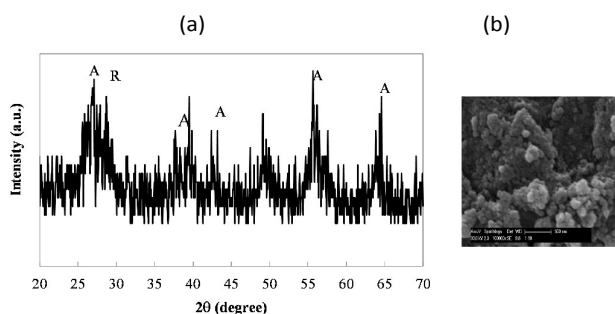


Fig. 3. (a) XRD diffraction pattern of the TiO_2 powder. A=Anatase, R=Rutile. (b) SEM images of unsupported TiO_2 .

Table 3. Some properties of TiO_2 catalyst

Phases	Phase percentage [%]	Specific Surface Area [m^2g^{-1}]	Band gap [eV]	Crystallite size [nm]
Anatase	60	54	3.00	12.8
Rutile	40			2.8

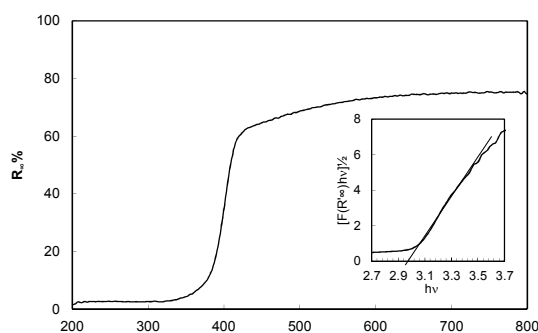


Fig. 4. Diffuse reflectance spectra of TiO_2 sample. Inset: plot of the square root of the modified Kubelka-Munk function vs. the energy of the absorbed light.

The specific surface area is $54 \text{ m}^2 \text{ g}^{-1}$, the particle sizes were 12.8 and 2.8 nm for anatase and rutile, respectively, and the band-gap value 3.00 eV. SEM micrographs (not shown for the sake of brevity) indicated that the TiO_2 sample presented irregular shapes and consisted of aggregates of particles whose size was ca. 60 nm (Fig.3b).

Membranes morphological and chemical characterization

Fig. 5 shows SEM images of Membrane 1. As it can be seen from Fig. 5b, many agglomerates of catalyst appearing as white spots are present through the membrane thickness, especially concentrated at the bottom surface, and no cavities are visible at this resolution. The presence of a higher concentration of catalyst in the DOWN surface with respect to the UP surface is related to sedimentation phenomena during the MeOH:H₂O solvent evaporation step of the polymeric solution. On the contrary, using EtOH:H₂O mixture as solvent

in the polymer solution (Membrane 2 and 3), a better dispersion of the catalyst in the Nafion membrane was observed (Fig. 6) owing to the higher capacity of the ethanol to disperse the catalyst in comparison to methanol.

Fig. 6 shows the SEM images of Membrane 2 cross section, both in SE and BSE mode (Fig. 6a and Fig. 6b, respectively). SE SEM image shows that, also in this case, the membrane is characterized by no cavities and some small catalyst agglomerates present through the membrane thickness. This was confirmed by BSE image, in which it is also possible to appreciate a relevant improvement of catalyst distribution with respect to Membrane 1, containing the same TiO_2 amount, despite a residual partial segregation on DOWN surface can be noticed. Fig. 7 shows BSE images of Membrane 3; in particular, Fig. 7b allows many catalyst agglomerates to be observed and again the partial catalyst segregation occurred at DOWN surface (Fig. 7b-c). This could be owed to an excessive amount of TiO_2 with respect to the polymeric matrix, causing its sedimentation during the solvent evaporation step of membrane formation. Also in this case, no visible cavities are present through the membrane thickness. The SEM images of the bare polymeric Nafion membrane not reported here, show that the membrane appears to be characterized by the absence of visible cavities. FT-IR spectroscopy analyses were carried out on both membrane surfaces.

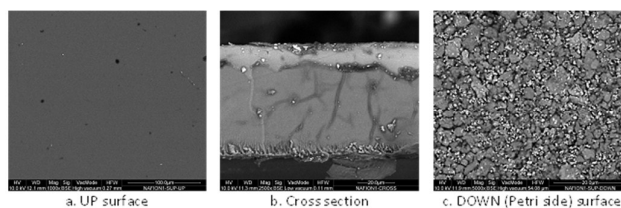


Fig. 5. Membrane 1 BSE SEM images (Mag: a. 1000x; b. 2500x; c. 5000x)

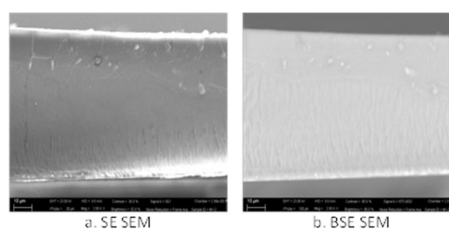


Fig. 6. Membrane 2 cross section SEM images (Mag: a. 2500x; b. 2500x)

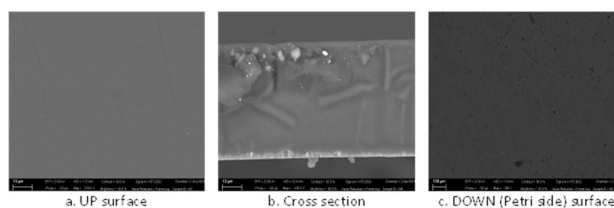


Fig. 7. Membrane 3 BSE SEM images (Mag: a. 3000x; b. 3000x; c. 200x)

Table 4. CO₂, CH₄ and H₂ permeances of Membrane 1 at 25°C and different RH.

RH, %	Permeance, dm ³ (STP) m h ⁻¹ m ⁻² bar ⁻¹		
	CO ₂	CH ₄	H ₂
0	4.41	6.96	9.19
100	2	1.6	3.4

To further confirm the integrity of the membranes, permeation measurements with single gas were also carried out in saturated conditions.

Table 4 summarizes the results for Membrane 1 which resulted to be dense and highly permeable to CO₂. The presence of water vapour reduced the permeance of all gases; however, CO₂ permeances remained high. Nafion membranes are well known in literature as proton transport^{26,27} membranes used in PEMFC with really good chemical stability. Nafion has hydrophilic domains favouring membrane hydration that, coupled with the high permeance of CO₂, assures the accessibility of reactants to the whole catalyst dispersed in the membrane.

Fig. 8 shows the spectra relative to the photocatalytic membranes (Membrane 1, 2 and 3). All the signals in the range between 970 and 1400 cm⁻¹ can be related to the Nafion structure. In particular, the bands appearing at 970–983 cm⁻¹ are attributed to C–O–C stretching vibrations; the band at ~1060 cm⁻¹ can be related to the symmetric stretching of –SO₃–. In the range between 1400 and 1100 cm⁻¹ the asymmetric stretching bands of –SO₃– should be found, but they are covered from the more intense bands of –CF₂ stretching, visible in the spectra.³⁵ Moreover, it can be seen that OH band intensity is higher for the DOWN surface spectrum with respect to the UP surface. This trend could be attributed to a higher TiO₂ concentration at the DOWN surface (Petri side), as observed in the SEM images (Fig. 5, Fig. 7).

As far as Membrane 3 is concerned (Fig. 8c), the signal relative to the OH band has a very different intensity for the UP and DOWN surface. This is certainly attributed to a high segregation of the catalyst at the DOWN surface of the membrane, because of the excessive TiO₂ amount. UV-Vis diffuse reflectance spectroscopy was performed on Membrane 4 and 1 in order to make a comparison between the bare Nafion membrane and that containing the photocatalyst and to verify its structural integrity when embedded inside the polymeric membrane. Membrane 4 gave a flat absorbance spectrum reported in Kubelka-Munk units (Fig. 9b) and obtained by processing the UV-Vis diffuse reflectance spectrum. It shows no absorbance maximum and it is characterized by a constant value of about 5 Kubelka-Munk units, owing to scattering phenomena. Kubelka-Munk absorbance spectrum relative to Membrane 1 (Fig. 9a), containing 1.2 wt% of TiO₂, presents an absorbance maximum of about 13 units in the range 280–300 nm, despite the catalyst segregation. This demonstrates that the catalyst maintains its structural integrity also when embedded inside the Nafion matrix, which in turn was proved to be transparent to UV radiation in the wavelength range considered, as the spectrum was recorded analysing the UP surface.

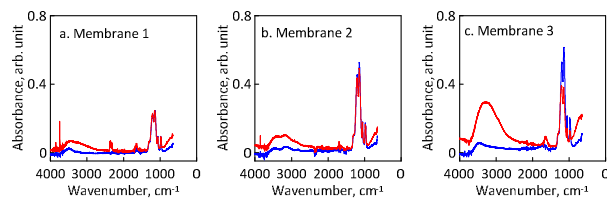


Fig. 8. FT-IR (ATR) spectra of UP membrane surface (blue lines) and DOWN membrane surface (red lines)

Photocatalytic reaction measurements

Different measurements were carried out in order to verify the photocatalytic activity of the membranes incorporating the catalyst. In all of them the error bar calculated was below 5%. Firstly, two photocatalytic experiments were performed testing Membrane 1 and varying the membrane side exposed to CO₂/H₂O feed stream and UV irradiation and as it was observed by means of the SEM and IR characterization the membrane had not symmetric catalyst distribution (Fig. 5b and c and Fig. 8a). Table 5 reports the photocatalytic experiments results relative to Membrane 1. In the first test performed, the membrane was placed into the module exposing its UP surface to the feed stream and UV radiation; whereas, in the second one the DOWN side of the membrane, richer in catalyst, was exposed. In both cases the photocatalytic reaction led to the evolution of CH₃OH as product, in the condensed aqueous phase. No CO and CH₄ were detected (the set up detection limit being 100 ppm).

No significant differences in MeOH yield and MeOH flow rate/TiO₂ weight were observed by performing the photocatalytic reduction of CO₂ exposing the two different surfaces. These results could be attributed to the fact that the Nafion polymer matrix is transparent to UV irradiation and therefore not only the superficial layer participates to the reaction, but also the inner layers. It has to be noticed that both CO₂ conversion and methanol yield have very low values; however, they results among the best by a comparison with the literature. In a second step, Membrane 2 was used to verify if the better catalyst distribution inside the bulk of the polymeric matrix (observed with SEM characterization, Fig. 6) could improve the performance of the photocatalytic membrane itself. In this case, the reaction measurements were carried out just exposing the UP surface as it was observed that the membrane surface exposed to retentate side does not influence the catalytic performances. One of the main problems related to the photocatalytic reduction of CO₂ is that it is often doubted that the products obtained could be developed from carbon impurities present in the reaction system in the first stage. In order to be sure that the products detected were not owing to impurities present in the photocatalytic membrane, the membrane was firstly subjected to “blank” reactions, with UV irradiation of Ar and H₂O stream in absence of CO₂, according to the operating conditions reported in Table 2. When performing the blank tests, some MeOH amounts were detected in the withdrawn samples (Fig. 10a). However, both MeOH wt% (not reported here) and “apparent” MeOH flow rate/TiO₂ weight (Fig. 10a) showed a clear decrease with run-time. This path should

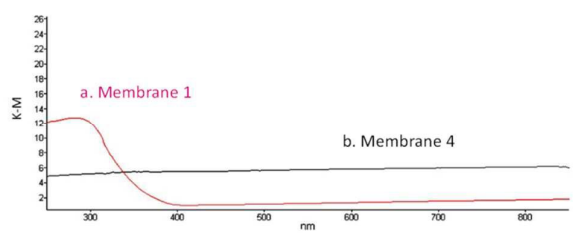


Fig. 9. Absorbance spectrum reported in Kubelka-Munk units

Table 5 – Reaction test results relative to Membrane 1.

	Membrane surface exposed	
	DOWN	UP
Reaction time, min	435	460
MeOH concentration, wt%	$1.20 \cdot 10^{-5}$	$1.34 \cdot 10^{-5}$
MeOH yield, %	$2.07 \cdot 10^{-5}$	$2.30 \cdot 10^{-5}$
MeOH flow rate/TiO ₂ weight, $\mu\text{mol g}_{\text{catalyst}}^{-1} \text{min}^{-1}$	0.092	0.10

indicate that some organic contaminants, probably owed to solvent residuals, were present in the polymeric matrix of the membrane giving the target product. Actually, the TOC measurements performed on the samples collected confirmed the presence of organics in amounts decreasing with run-time. The correspondent weight percentage resulted to be very low (Fig. 10b) but anyway almost two orders of magnitude higher than that of the detected methanol. However, when switching the feeding gas from Ar to CO₂, real MeOH flow rate/TiO₂ weight suddenly increased, reaching a maximum of $0.73 \mu\text{mol g}_{\text{catalyst}}^{-1} \text{min}^{-1}$. The increasing trend of MeOH flow rate/TiO₂ weight during reaction and its decreasing in blank tests are indexes of methanol production by CO₂ conversion. In addition, this value resulted to be over 7 times higher with respect to that obtained with Membrane 1, confirming that the better catalyst distribution characterizing Membrane 2 had a positive effect on the catalytic performance of the membrane itself. Membrane 3 was tested following the previous procedure, which is feeding Ar until MeOH was not longer measured. Then, CO₂ replaced Ar in the feed and real MeOH production was observed. MeOH concentration remained almost constant with respect to the test carried out by using Membrane 2, but MeOH flow rate/TiO₂ weight showed a significant decrease (Fig. 11a), being about 3 times lower. This behaviour could be explained by considering that the increase of the amount of catalyst embedded inside the membrane, caused segregation and this phenomenon could have negatively influenced the performances of the catalytic membrane itself. Actually, catalyst aggregation could have not allowed an effective interaction between TiO₂ particles and UV light. Moreover MeOH, in the presence of a higher amount of TiO₂ in the Membrane 3, could react. Also in this case, the TOC content in the samples resulted to be much higher with respect to MeOH content (Fig. 11b). The same tests were also carried out on Membrane 4, which is to say on the bare Nafion, in order to prove that the polymeric matrix does not possess photocatalytic activity by itself.

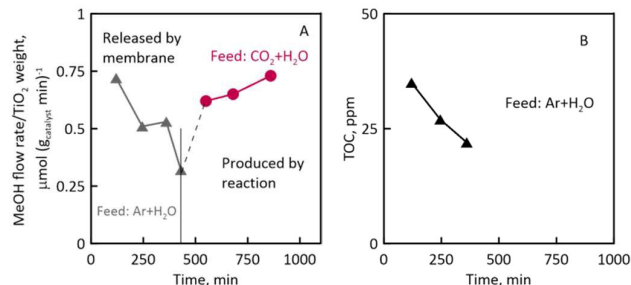


Fig. 10. Photocatalytic experiments results using Membrane 2

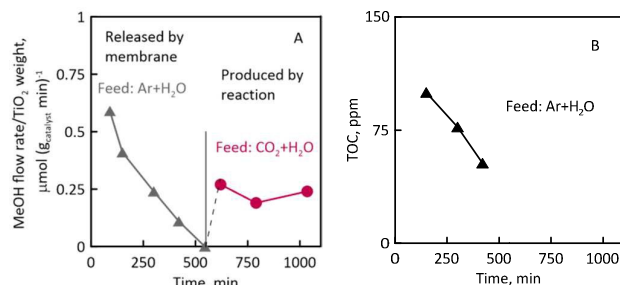


Fig. 11. Photocatalytic experiments results using Membrane 3

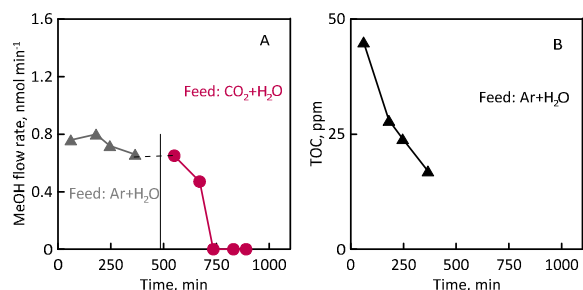


Fig. 12. Photocatalytic experiments results using Membrane 4

As it can be observed in Fig. 12, MeOH flow rate in the samples and TOC weight percentage reduced with time. In particular MeOH content decreased to zero after 750 minutes of irradiation, even after switching the feed from Ar to CO₂. This path proves that Nafion does not possess any catalytic activity and probably, as Membrane 4 was prepared by using MeOH as the co-solvent, a small residual MeOH amount were released by the membrane during the occurrence of the test. Fig. 13 summarizes the results obtained relative to MeOH flow rate/TiO₂ weight, considering both the quality distribution of catalyst and its content inside the membrane. At equal TiO₂ amount (1.2 wt% in the membrane), a better distribution, relative to Membrane 2 (labelled in Fig. 13 as “well dispersed”) as proved by means of SEM imaging (Fig. 6), resulted to increase the MeOH flow rate/TiO₂ weight with respect to Membrane 1. In this last case, the only difference was owed to the partial catalyst deposition (Fig. 5). Increasing the catalyst amount to 5 wt% produced again its partial segregation (Fig. 7) and caused a significant decrease of the photocatalytic performances of the membrane. The visible pinky background highlights the transparency of Membrane 2 owing to the good catalyst dispersion. On the contrary, the other membranes did not show similar transparency owing to catalyst segregation.

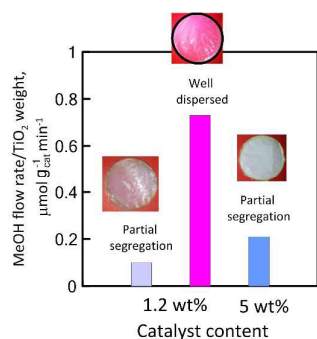


Fig. 13. MeOH flow rate/TiO₂ weight as a function of catalyst content percentage in the polymeric membrane.

Consequently, the partial catalyst deposition on DOWN surface of the membrane and the presence of aggregates seem to be crucial parameters for the membrane efficiency and some strategies should be attempted in order to improve the catalyst distribution also at higher content. Such strategies could comprise the reduction of membrane formation time by accelerating solvent evaporation (e.g. higher temperature or gas sweeping), TiO₂ functionalization with surfactants or use of different polymeric material.

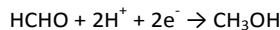
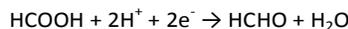
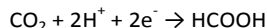
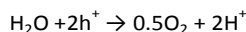
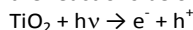
Nevertheless, even with the current conditions used, MeOH flow rate/TiO₂ weight resulted to be comparable or even much higher with respect to that found in other works present in literature (Table 6), the best results being obtained by Pathak et al.³² by immobilizing TiO₂ into commercial Nafion membranes and by using liquid CO₂ in supercritical conditions as feed.

In the present work a very high MeOH flow rate/TiO₂ weight was obtained under mild operating conditions (atmospheric pressure, room temperature and gaseous CO₂ as feed); the best results were observed by using Membrane 2.

The photocatalytic CO₂ reduction mechanism is very complex and still unclear. Many hypotheses were advanced on the formation of the various products deriving from CO₂.³⁶⁻³⁸ Generally the compounds formed during the gaseous photocatalytic CO₂ reduction were CO and CH₄^{39,40} whilst formic acid, formaldehyde and methanol were mainly observed during liquid phase runs.⁴¹⁻⁴⁴

Published papers^{39,43,44} dealing with batch reactors operating in similar conditions for CO₂ photo-oxidation over TiO₂ catalyst showed methane as the main reaction product and trace of formic acid. It is worth of note that, differently from what can be found in most of the literature, in this work neither CH₄ nor CO were detected, methanol being the main product obtained. This can probably be attributed to the synergic effect of the use of membranes inside which the photocatalyst was embedded and a continuous flow mode reactor to carry out the reaction of CO₂ and H₂O. Actually, avoiding the use of a batch reactor, the substrate undergoes a lower degree of reduction as fresh CO₂ is continuously fed into the system and the produced methanol is continuously removed from the catalytic sites reducing the possibility to have over oxidation phenomena.³⁹ Ion chromatography analyses, performed on selected samples, revealed that traces amount of formic acid were formed in the presence of Membrane 2. Methanol formation is a multi-electronic process which, in the presence

of TiO₂ and H₂O, can take place in different stages according to the reactions below reported (adapted from literature data):



The circumstance that in our system formic acid and formaldehydes are not detected, or are present in low amounts in the case of HCOOH with Membrane 2, can be explained by the fast reaction rate of these compounds to form MeOH or by the direct methanol formation. Moreover, the continuous removal of methanol from reaction volume avoids its oxidation.

As overall consideration it can be seen that the yield of methanol and thus CO₂ conversion are very low, if evaluated as absolute values, even if resulted among the best in literature. It has to be considered that this process is at a very early stage of development and it needs more and more efforts to make it profitable. However, it remains highly promising and attractive as it has the great advantage of being completely green using CO₂ and water as reactants exploiting sunlight as energy source to produce liquid fuels.

Conclusions

In this work, photocatalytic CO₂ conversion to methanol was carried out in a continuous membrane reactor with a TiO₂-based membrane irradiated by UV light.

Various photocatalytic membranes were prepared embedding TiO₂ catalyst inside a polymeric Nafion matrix. A good distribution of catalyst was achieved by choosing an appropriate co-solvent for the preparation of the polymeric solution (e.g. EtOH) at a chosen catalyst amount of 1.2 wt%.

By using the membrane 2, the one with the best TiO₂ distribution, no CH₄ nor CO formation were observed whereas a MeOH flow rate/TiO₂ weight of 45 μmol (g_{catalyst} h)⁻¹ was obtained under mild experimental conditions. According to authors knowledge, such a value is a relevant advance over the existing literature as it is higher than most of the data, also using supercritical CO₂, reported up to date.

Moreover, it was observed that the catalytic performances were strictly related to the membrane preparation, as the higher methanol flow rate/TiO₂ weight was achieved by using the photocatalytic membrane (Membrane 2) with the best catalyst distribution even if with a lower content (Membrane 3). Comparing the results with bare Nafion membrane, it was demonstrated that the polymeric matrix does not possess any photocatalytic activity by itself and, thus, the whole methanol produced has to be attributed to the presence of catalyst dispersed in the Nafion matrix.

The present work demonstrates that the use of photocatalytic Nafion membranes has a wide range of improvement and could be a promising candidate for an advanced route of CO₂ conversion in CH₃OH.

Table 6. Comparison of results reported in literature

Catalyst	Reactor configuration	MeOH flow rate/catalyst weight	CH ₄ , CO, etc. flow rate/catalyst weight	Ref.
		$\mu\text{mol (g}_{\text{catalyst}} \text{ h)}^{-1}$	$\mu\text{mol (g}_{\text{catalyst}} \text{ h)}^{-1}$	
TiO ₂ /Y-zeolite anchored on Vycor glass	Batch	5	8 CH ₄	45
Ti-mesoporous zeolite	Batch	3.5	7.5 CH ₄	46
Ti-b(OH) and Ti-b(F)	Batch	5.9	1 CH ₄	47
TiO ₂ and 2% Cu/TiO ₂ in NaOH solution	Batch	0.78 for TiO ₂ 19.75 for Cu/TiO ₂	-	48
Cu/TiO ₂ film supported on optical-fiber	Continuous	0.45	-	49
Cu/TiO ₂ and Ag/TiO ₂ film supported on optical-fiber	Continuous	4.12	-	5
TiO ₂ anatase	Batch	0.075	0.40 CH ₄	6
TiO ₂ polymorphs	Continuous	-	3.15 CO; 2.13 CH ₄	50
TiO ₂ polymorphs	Continuous	-	2.1 CO	11
phtalocyanines/TiO ₂	Batch	-	26 HCOOH	43
TiO ₂ nanoparticles in porous cavities of commercial Nafion membranes	Continuous	56 (using supercritical CO ₂ as feed)	38 HCOOH 6 CH ₃ COOH	32
TiO ₂ nanoparticles in Nafion membrane	Continuous	45 (Membrane 2) 12.6 (Membrane 3)	Traces of HCOOH (Membrane 2)	This work

Acknowledgements

The research project PON 01_02257 "FotoRiduCO₂ - Photoconversion of CO₂ to methanol fuel", co-funded by MIUR (Ministry of University Research of Italy) with Decreto 930/RIC 09-11-2011 in the framework the PON "Ricerca e competitività 2007-2013", is gratefully acknowledged

References

- https://co2.earth/global-co2-emissions. Last Access: 27/01/2016
- A. Brunetti, F. Scura, G. Barbieri G., Drioli E., Journal of Membrane Science, 2010, 359, 115-125. dx.doi.org/10.1016/j.memsci.2009.11.040
- S.C. Roy, O.K. Varghese, M. Paulose and C.A. Grimes, ACS Nano, 2010, 4, 1259-1278.
- A. Dhakshinamoorthy, S. Navalon, A. Corma and H. Garcia, Energy & Environmental Science, 2012, 5, 9217-9233.
- J.C.S. Wu, Catalysis Surveys from Asia, 2009, 13, 30-40.
- K. Kočí, L. Obalová, L. Matějová, D. Plachá, Z. Lacný, J. Jirkovský and O. Šolcová, Applied Catalysis B: Environmental, 2009, 89, 494-502.
- T. Inoue, A. Fujishima, S. Konishi, K. Honda, Nature, 1979, 277, 637-640.
- J.C. Hemminger, R. Carr and G.A. Somorjai, Chemical Physical Letters, 1978, 57, 100-108.
- S. Das, W.M.A. Wan Daud, RSC Advances, 2014, 4, 20856-20893.
- K. Kočí, L. Obalová, Z. Lacný, Chemical Papers, 2008, 62, 1-9.
- H. Zhao, L. Liu, J.M. Andino and Y. Li, Journal of Materials Chemistry A, 2013, 1, 8209-8216
- R. Molinari, M. Mungari, E. Drioli, A. Di Paola, V. Loddo, L. Palmisano, M. Schiavello, Catalysis Today, 2000, 55, 71-78.
- R. Molinari, L. Palmisano, E. Drioli, M. Schiavello, Journal of Membrane Science, 2002, 206, 399-415.
- H. Choi, E. Stathatos, D.D. Dionysiou, Desalination, 2007, 202, 199-206.
- H. Choi, A.C. Sofranko and D.D. Dionysiou, Advanced Functional Materials, 2006, 16, 1067-1074.
- A. Pandikumar, S. Murugesan, R. Ramaraj, ACS Applied Materials and Interfaces, 2010, 2, 1912-1917.
- C. Pandiyarajan, A. Pandikumar, R. Ramaraj, Nanotechnology, 2013, 24, 435401.
- A. Pandikumar, S. Manonmari, R. Ramaraj, Catalysis Science and Technology, 2012, 2, 345-353.
- A. Pandikumar, R. Ramaraj, Journal of Hazardous Materials, 2012, 203-204, 244-250.
- I.R. Bellobono, B. Barni, F. Gianturco, Journal of Membrane Science, 1995, 102, 139-147.
- A. Barni, A. Cavicchioli, E. Riva, L. Zanoni, F. Bignoli, I.R. Bellobono, F. Gianturco, A. De Giorgi, H. Muntau, L. Montanarella, S. Facchetti, L. Castellano, Chemosphere, 1995, 30, 10, 1861-1874.
- H. Dzinun, M.H.D. Othman, A.F. Ismail, M.H. Puteh, M.A. Rahman and J. Jaafar, Chemical Engineering Journal, 2015, 269, 255-261.
- S. Leong, A. Razmjou, K. Wang, K. Hapgood, X. Zhang, Journal of Membrane Science, 2014, 472, 167-184.
- P. Liu, J. Bandara, Y. Lin, D. Elgin, L.F. Allard and Y.P. Sun, Langmuir, 2002, 18, 10398-10401.
- Y.P. Sun, P. Atornjitjawat, Y. Lin, P. Liu, P. Pathak, J. Bandara, D. Elgin, M. Zhang, Journal of Membrane Science, 2004, 245, 211-217.
- H. Miyoshi, S. Nippa, H. Uchida, H. Mori and H. Yoneyama, Bulletin of the Chemical Society of Japan, 1990, 63, 12, 3380-3384.
- K.A. Mauritz, R.B. Moore, Chem. Rev. 2004, 104, 4535-4585
- E. Drioli, E. Fontananova, Annual Review of Chemical and Biomolecular Engineering, 2012, 3, 395-420
- F.R.F. Fan, H.Y. Liu and A.J. Bard, The Journal of Physical Chemistry, 1985, 89, 4418-4420.
- A. Yaron and L. Arcan, Thin Solid Films, 1990, 185, 181-188.
- J. Premkumar and R. Ramaraj, Journal of Photochemistry and Photobiology A: Chemistry, 1997, 110, 53-58.
- P. Pathak, M.J. Meziani, Y. Li, L.T. Cureton and Y.P. Sun, Chemical Communication, 2004, 1234-1235.
- P. Pathak, M.J. Meziani, L. Castillo and Y.P. Sun, Green Chemistry, 2005, 7, 667-670.
- H. Zhang, J.F. Banfield, The Journal of Physical Chemistry B, 2000, 104, 3481-3487.
- Z. Liang, W. Chen, J. Liu, S. Wang, Z. Zhou, W. Li, G. Suna, Q. Xin, Journal of Membrane Science, 2004, 233, 39-44.

ARTICLE

Journal Name

- 36 G. R. Dey, *Journal of Natural Gas Chemistry*, 2007, 16, 217-226.
- 37 S. N. Habisreutinger, L. Schmidt-Mende, J. K. Stolarczyk, *Angewandte Chemie International Edition*, 2013, 52, 2–39.
- 38 Y. Izumi, *Coordination Chemistry Reviews*, 2013, 257, 171–186.
- 39 M. Bellardita, A. Di Paola, E. García-López, V. Loddo, G. Marci, L. Palmisano, *Current Organic Chemistry*, 2013, 17, 2440-2448.
- 40 W. Lin, H. Han, H. Frei, *The Journal of Physical Chemistry B*, 2004, 108, 18269-18273.
- 41 G. Qin, Y. Zhang, X. Ke, X. Tong, Z. Sun, M. Liang, S. Xue, *Applied Catalysis B: Environmental*, 2013, 129, 599–605.
- 42 Slamet, H.W. Nasution, E. Purnama, S. Kosela, J. Gunlazuardi, *Catalysis Communications*, 2005, 6, 313–319.
- 43 G. Mele, C. Annese, A. De Riccardis, C. Fusco, L. Palmisano, G. Vasapollo, L. D'Accolti, *Applied Catalysis A: General*, 2014, 481, 169–172.
- 44 G. Mele, C. Annese, L. D'Accolti, A. De Riccardis, C. Fusco, L. Palmisano, A. Scarlino, G. Vasapollo, *Molecules*, 2015, 20, 396-415.
- 45 M. Anpo, H. Yamashita, Y. Ichihashi, Y. Fujii and M. Honda, *The Journal of Physical Chemistry*, 1997, 101, 2632-2636.
- 46 H. Yamashita, Y. Fujii, Y. Ichihashi, S.G. Zhang, K. Ikeue, D.R. Park, K. Koyano, T. Tatsumi, M. Anpo, *Catalysis Today*, 1998, 45, 221-227.
- 47 K. Ikeue, H. Yamashita and M. Anpo, *The Journal of Physical Chemistry B*, 2001, 105, 8350-8355.
- 48 I-H. Tseng, W.C. Chang, J.C.S. Wu, *Applied catalysis B: Environmental*, 2002, 37, 37-48.
- 49 J.C.S. Wu, H.M. Lin, C.L. Lai, *Applied Catalysis A: General*, 2005, 296, 194-200.
- 50 L. Liu, H. Zhao, J.M. Andino and Y. Li, *ACS Catalysis*, 2012, 2, 1817-1828.

Textual abstract

Metanol was produced by CO₂ photocatalytic reduction over by TiO₂- Nafion-based membranes by using a continuous flow membrane reactor. A MeOH flow rate/TiO₂ weight of 45 μmol (g_{catalyst} h)⁻¹ was measured operating at 2 bar of feed pressure. So far, this value results to be higher than the most of the literature data reported up to date. Moreover, MeOH production is considered as a relevant advance over the existing literature results mostly proposing CH₄ as reaction products.

Graphical Abstract

